*minerals*

MDPI

*Article*

# Detrital Zircon Provenance of the Cenozoic Sequence, Kotli, Northwestern Himalaya, Pakistan; Implications for India–Asia Collision

**Muhammad Awais [1,2], Muhammad Qasim [2,3,4,*,†,‡], Javed Iqbal Tanoli [3,*,‡], Lin Ding [2,4,†], Maryam Sattar [5], Mirza Shahid Baig [6] and Shahab Pervaiz [6]**

1 State Key Laboratory of Lithospheric Evolution, Institute of Geology and Geophysics, Chinese Academy of Sciences, Beijing 100029, China; awaiskhan@mail.iggcas.ac.cn
2 University of Chinese Academy of Sciences, Beijing 100049, China; dinglin@itpcas.ac.cn
3 Department of Earth Sciences, COMSATS University Islamabad, Abbottabad Campus, Abbottabad 22010, Pakistan
4 Key Laboratory of Continental Collision and Plateau Uplift, Institute of Tibetan Plateau Research, and Center for Excellence in Tibetan Plateau Earth Sciences, Chinese Academy of Sciences, Beijing 100101, China
5 Institute of Space Technology, Islamabad 44000, Pakistan; msattar@ist.edu.pk
6 Institute of Geology, University of Azad Jammu and Kashmir, Muzaffarabad 13100, Pakistan; drshahidbaig@yahoo.com (M.S.B.); geo_shahab@yahoo.com (S.P.)
* Correspondence: qasimtanoli@itpcas.ac.cn or qasimtanoli@cuiatd.edu.pk (M.Q.); javed_iqbal@cuiatd.edu.pk (J.I.T.)
† Current address: Institute of Tibetan Plateau Research, Chinese Academy of Sciences, Building 3, Courtyard 16, Lin Cui Road, Chaoyang District, Beijing 100101, China.
‡ Current address: Department of Earth Sciences, COMSATS University Islamabad, Abbottabad Campus, University Road, Tobe Camp, Abbottabad 22044, Pakistan.



**Citation:** Awais, M.; Qasim, M.; Tanoli, J.I.; Ding, L.; Sattar, M.; Baig, M.S.; Pervaiz, S. Detrital Zircon Provenance of the Cenozoic Sequence, Kotli, Northwestern Himalaya, Pakistan; Implications for India–Asia Collision. *Minerals* **2021**, *11*, 1399. https://doi.org/10.3390/min11121399

Academic Editors: David Gómez-Gras and Marta Roigé

Received: 15 October 2021
Accepted: 7 December 2021
Published: 11 December 2021



**Abstract:** This study reported the detrital zircon U-Pb geochronology of the Cenozoic sequence exposed in Kotli, northwestern Himalaya, Pakistan, which forms part of the Kashmir foreland basin. The U-Pb detrital age patterns of the Paleocene Patala Formation show a major age cluster between ~130–290 Ma, ~500–1000 Ma and ~1000–1500 Ma, which mainly resembles the lesser and higher Himalayan sequence. However, the younger age pattern (~130–290 Ma) can be matched to the ages of the ophiolites exposed along the Indus–Tsangpo suture zone. In addition, two younger grains with 57 Ma and 55 Ma ages may indicate a contribution from the Kohistan-Ladakh arc. The detrital zircons in the upper Tertiary sequence show the increased input of younger detrital ages <100 Ma, with more pronounced peaks at ~36–58 Ma, ~72–94 Ma and ~102–166 Ma, indicating the strong resemblance to the Asian sources including the Kohistan–Ladakh arc, Karakoram block and Gangdese batholith. This provenance shift, recorded in the upper portion of Patala Formation and becoming more visible in the upper Tertiary clastic sequence (Kuldana and Murree formations), is related to the collision of the Indian and Asian plates in the northwestern Himalayas. Considering the age of the Patala Formation, we suggest that the Indian and Asian plates collided during 57–55 Ma in the northwestern Himalayas, Pakistan.

**Keywords:** detrital zircon provenance; Cenozoic sequence; Hazara-Kashmir syntaxis; Kashmir foreland–fold belt; northwestern Himalaya; India–Asia collision

## 1. Introduction

The Himalayan orogenic system, which is the result of the Cenozoic India–Asia collision, is a natural laboratory to study continent–continent collisional tectonics. In response to the collision, a foreland basin system was developed on the northern margin of the Indian plate, which received the detritus from the Indian and Asian blocks. The Himalayan foreland basin occupied the Sub-Himalayan region, which consists of Paleocene–Eocene marine rocks unconformably overlain by Oligocene and younger fluvial sediments throughout the orogen.

The mixing of the India–Asia detritus provides minimal age constraints on the timing of collision. The timing and location of the India–Asia collision has remained a hotly debated topic in the last two decades, which resulted in a wide range of collision ages along the strike [1]. This difference in the collision age is due to various methods adopted to constrain the collision timing. These methods consisted of dating of the magmatic arc record [2], dating of ultra-high-pressure eclogite associated with subduction zone [3–6], the overlapping of paleo-latitudes [7–10], changes in the velocity of Indian plate [11], cessation of marine facies [12], faunal migration across the plates and sedimentary provenance [4,13–17]. As collision is a process in which the first stage is the ophiolite obduction, and the last stage is the cessation of marine facies, these different methods can be used to date each stage of the collision process. However, the difference in the collision age can be seen through a similar proxy along strike points towards a diachronous collision [18], with the timing of collision reported in the northwestern Himalaya ranging from ~65–34 Ma [19–21]. However, a recent study in the Balakot area proposed the collision to be at ~56–55 Ma [16]. The latter study provides important evidence for the collision age, such as the provenance change, the mixing of India–Asia detritus and the recognition of disconformity at the Paleocene–Eocene boundary. Therefore, in this study, we have selected an area southeast of the Balakot in the same basin to study the Cenozoic sequence for stratigraphic characterization and their tectonic implications in relation to the India–Asia collision.

The study area is part of the sub-Himalayas and is located in the Hazara-Kashmir syntaxial region in its eastern proximity, as shown in Figure 1A,B [22]. The area comprises the exposed sequence of the Indian plate, which is intensely deformed as reflected by the regional-scale folds and faults.

U-Pb detrital zircon geochronology is applied on selected samples to interpret the provenance for constraining the collision timing between the Indian and Asian plates in northwestern Himalayas, Pakistan (Figure 1C).

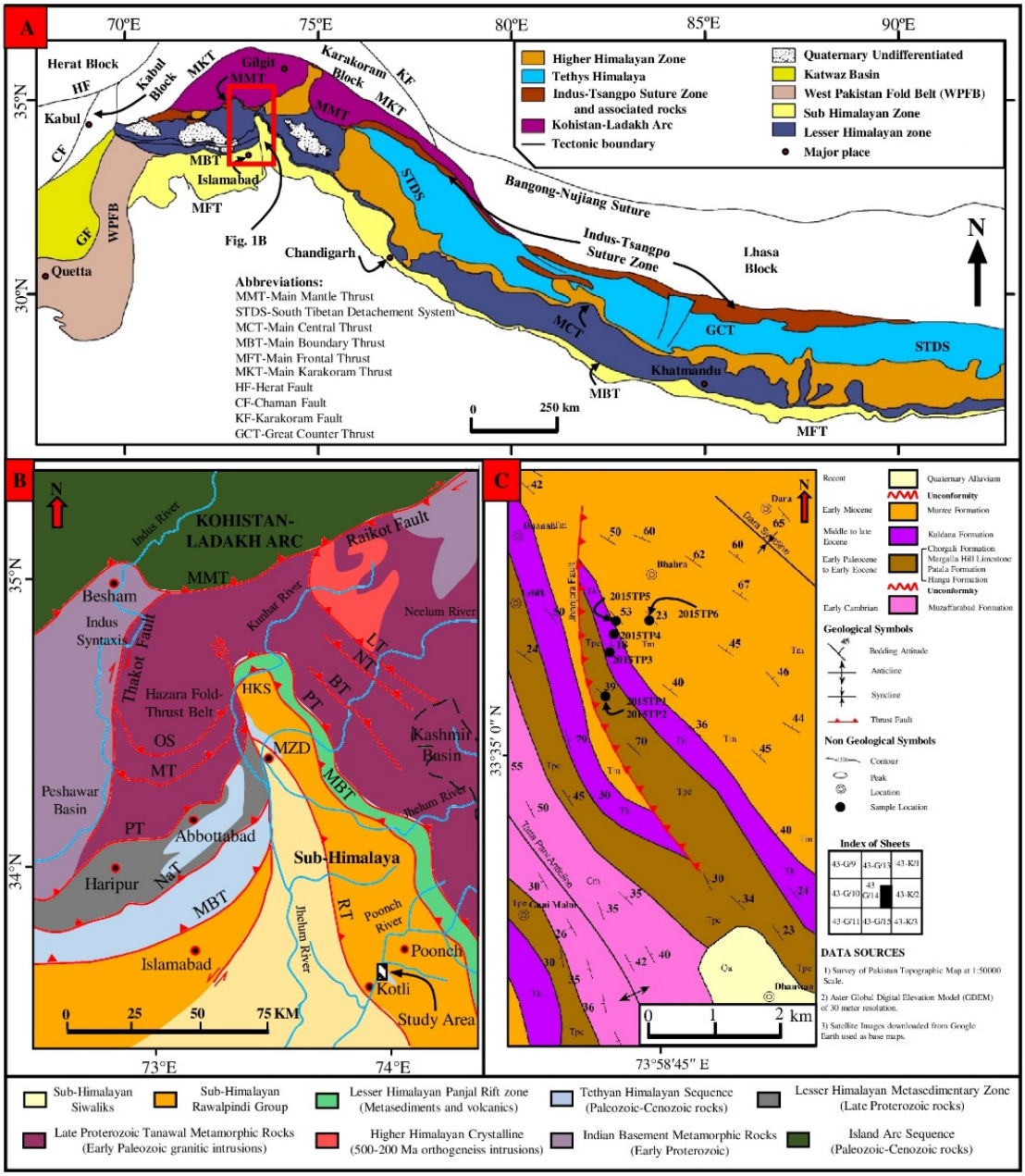


**Figure 1.** (**A**) Generalized Tectonic map showing major tectonostratigraphic zones (modified after Qasim et al., [17] and based on many sources references therein). The red rectangle shows the extent of Figure 1B. (**B**) Simplified Tectonic map of Hazara-Kashmir syntaxis and surrounding areas (after Qasim et al. [17] and references therein). The hatched black rectangle shows the location of the studied area. MMT—Main Mantle Thrust, LT—Laut Thrust, NT—Neelum Thrust, BT—Barian Thrust, PT—Panjal Thrust, HKS—Hazara Kashmir Syntaxis, MBT—Main Boundary Thrust, MZD—Muzaffarabad, OS—Oghi Shear zone, MT—Mansehra Thrust, NaT—Nathia Gali Thrust and RT—Riasi Thrust. (**C**) Geological and structural map of the studied area showing stratigraphic units and location of samples collected for U-Pb geochronology.

## 2. Regional Tectonic Setting

The three major tectonic blocks, i.e., Indian Plate, Eurasian Plate and Kohistan-Ladakh Arc (KLA), are involved in controlling the tectonics of the northwestern Himalayas (Figure 1A). The KLA is sandwiched between the Indian and Eurasian Plates. It is an intra-oceanic island arc that first collided along the Main Karakoram Thrust (MKT) with Eurasian Plate, forming a northern suture zone during the Late Cretaceous period [23]. The collision of KIA with the Indian Plate occurred during the Early to Middle Eocene along Main Mantle Thrust, forming the southern suture zone [23,24]. During this collision, the Tethys

Ocean closed, and the remnants of the oceanic lithosphere were exposed along the suture zone as ophiolites. These ophiolites were emplaced during the Cretaceous and Paleocene periods onto the northern Indian margin and thus indicate the initiation of the collision process [25]. These ophiolites are located from west to east along the strike. They are named: Bela-Muslimbagh-Zhob ophiolites, Waziristan Ophiolites, Dargai Ophiolites, Jijal and Chilas complexes, Spontong ophiolites, Nidar ophiolites and Xigaze ophiolites [26]. The sequences of KIA obducted onto the Indian Plate rocks are due to this Eocene collision. This Eocene collision is responsible for the formation of the northwestern Himalayas in Kashmir. Generally, the Himalayan mountain ranges are divided into four tectonostratigraphic sub-divisions separated by boundary faults [27]. These four tectonostratigraphic sub-divisions comprise the Tethyan Himalaya, Greater Himalaya, Lesser Himalaya and sub-Himalaya. The boundary faults which separated these blocks from each other (north to south) include the South Tibetan Detachment System (STDS), Main Central Thrust (MCT), Main Boundary Thrust (MBT) and Main Frontal Thrust (MFT), respectively.

The study area occupying the position within the Hazara-Kashmir syntaxial region at the eastern flank is part of the sub-Himalayas. The sub-Himalayas consists of folded Neogene mollasses sediments, which are covered by alluvium in the south. In the foothill region of sub-Himalaya, an active Himalayan Frontal Fault cuts this Indo–Gangetic alluvium [28]. A series of en-echelon faults parallel to the strike of the orogen between Punjab and Assam are noted along this frontal fault [29,30]. This frontal fault is terminated with MBT on the western side of the syntaxis [22]. The major thrust faults form a loop near Paras and form an antiformal structure named the Hazara-Kashmir syntaxis (HKS). These faults include the Main Boundary Thrust (MBT), Panjal Fault and Main Central Thrust (MCT). The Miocene molasses in the axial zone of HKS is a continuation of the sub-Himalayan zone towards the southeast [28].

## 3. Stratigraphy

The regional stratigraphy of the Kashmir basin comprises of pre-Cambrian to Recent sedimentary and meta-sedimentary rocks [31]. The stratigraphic succession of the Kashmir basin is broadly divided into basement and cover sequences. The basement belongs to the pre-Cambrian Dogra Slates in the Kashmir basin, which are equivalent to the Hazara Formation, Manki Slates and Landikotal Slates. The cover sequence includes Early Paleozoic and Cenozoic rocks. Two major hiatuses exist in succession, one of them is at the boundary of basement rocks and cover sequence, and the other is between the Early Paleozoic and Cenozoic sequences.

The stratigraphy of the mapped area consists of lithological units of the cover sequence. The basement rocks are not exposed in the mapped area. These lithological units comprise the Early Paleozoic Muzaffarabad Formation and Tertiary rocks. The Tertiary sequence comprises of Hangu and Patala formations of the Paleocene age, Margalla Hill Limestone, Chorgali and Kuldana formations of the Eocene age, Murree Formation of Miocene age and some Quaternary deposits (Figures 1C and 2). These lithological units are described in detail in the following sections.

### *3.1. Muzaffarabad Formation*

Various stratigraphic names have been given to the Muzaffarabad Formation [32] in different parts of the Lesser and sub-Himalayas, such as Sirban Limestone [33], Great Limestone [34] and Jammu Limestone [35,36]. The main lithologies of the Muzaffarabad Formation include dolomite (cherty and/or stromatolitic), black limestone, chert bands and quartzite. The dolomite is fine to medium grained and hard. It shows chop board weathering (Figure 3A) and solutioning. It has sharp contact with fine to medium-grained quartzite. The Muzaffarabad Formation is the oldest exposed unit in the study area. Therefore, its contact with underlying units is buried, while the contact with the overlying Hangu Formation is marked by a regional unconformity. The age assigned to the Muzaffarabad Formation is Cambrian.

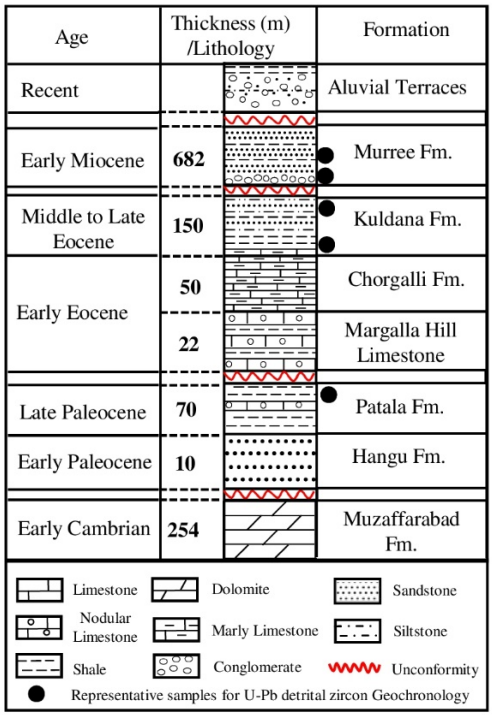


**Figure 2.** Stratigraphic column of the studied area showing position of the samples collected for U-Pb geochronology.

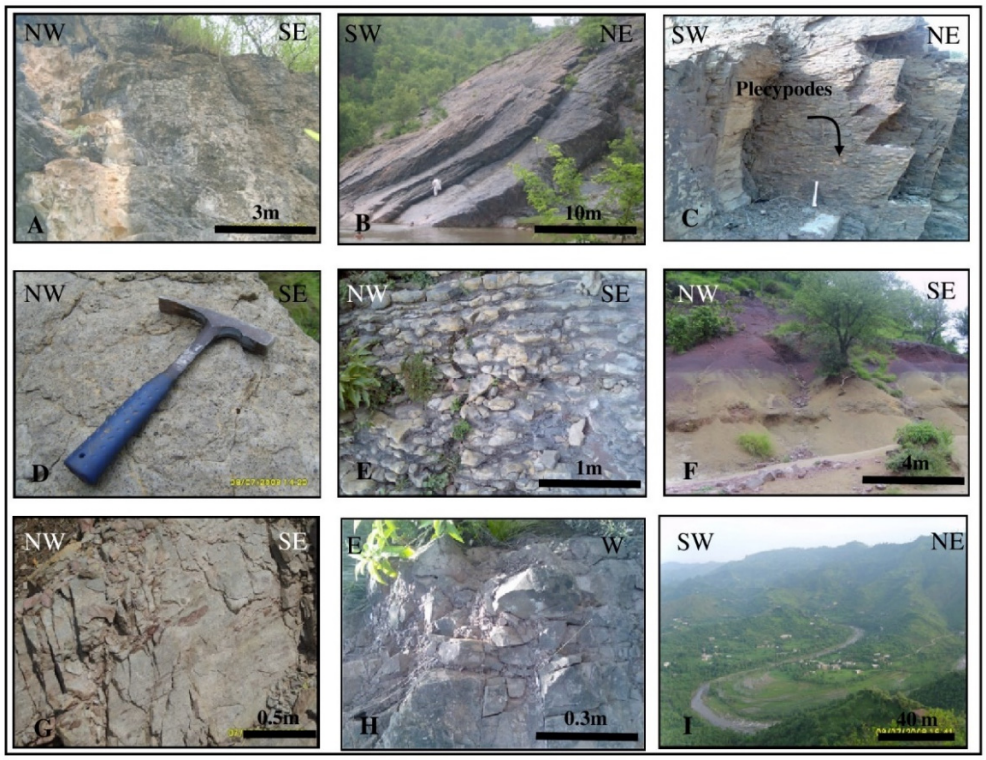


**Figure 3.** (**A**) The dolomite of Muzaffarabad Formation showing chop board weathering. (**B**) The bauxite and clay of the Hungu Formation are exposed in the Dandli area. (**C**) Plecypodic beds in shaly limestone of Patala Formation exposed near Gradh junction. (**D**) The shales of Margalla Hill Limestone showing larger forams. (**E**) Thinly bedded nodular limestone with alternate shales of Chorgalli Formation exposed near Gradh. (**F**) Variegated shales of Kuldana Formation exposed at Bhabra. (**G**) Fractured and jointed sandstone of Murree Formation exposed near Dara area. (**H**) Rip ups in the Murree Formation. (**I**) Cultivated river terraces in the Dandli area.

### *3.2. Hangu Formation*

The Hangu Formation comprises laterite, bauxite, fireclay (Figure 3B), ferruginous sandstone and coal seam. The weathered color of bauxite is rusty brown. The Hangu Formation overlies the Muzaffarabad Formation of the Cambrian age, thus forming lower contact unconformable. Similarly, the contact with the overlying Patala Formation is also unconformable. The age of the Hangu Formation is Early Paleocene.

### *3.3. Patala Formation*

The Patala Formation consists dominantly of shales. However, subordinate limestone beds and sandstone are also present. The color of shales varies from khaki, brown and grey. The shale appeared thinly laminated and splintery. The color of the limestone is dull grey on the weathered surface, and grey to light grey color on a fresh surface. It is fine-grained, thinly bedded and soft. The limestone has Pelecypodic beds near the Gradh junction (Figure 3C). The coal seams are found at some places in the Dandli area. The lower contact of the Patala Formation with the Hangu Formation is unconformable, and the upper contact with the Margalla Hill Limestone is gradational. However, in the upper part of the Patala Formation, the paleosol layer is present below the contact with Margalla Hill Limestone. This paleosol layer may represent the Paleocene–Eocene unconformity. The age of the Patala Formation is Late Paleocene.

### *3.4. Margalla Hill Limestone*

The Margalla Hill Limestone mainly comprises nodular limestone with minor shale intercalations. The limestone is medium to thick-bedded, nodular, fine-grained and hard. The weathered surface of limestone exhibits dull grey to light grey color while the fresh surface shows a dark grey color. The size of the nodule varies from 20 cm to 30 cm. The limestone is richly fossiliferous. The abundant fossils present in the limestone belong to the foraminiferas (Figure 3D). The lower contact of Margalla Hill Limestone with the Patala Formation is gradational, and the upper contact with the Chorgali Formation is conformable gradational. The age of the Margalla Hill Limestone is Early Eocene.

### *3.5. Chorgali Formation*

The Chorgali Formation comprises shales, limestone and quartzite. Shales are present in the lower unit. The color of shale is grey to dark grey and blackish. The limestone of the Chorgali Formation shows platy nodularity (Figure 3E). The nodule's size (10 cm) is smaller than the size (30 cm) of the nodules of the Margalla Hill Limestone. The limestone is thinly bedded and white to light grey in color. The fresh color of the limestone is dark grey to black. The lower contact of the Chorgali Formation with the Margalla Hill Limestone is gradational and upper contact with the Kuldana Formation is conformable. The age of the Chorgali Formation is Early Eocene.

### *3.6. Kuldana Formation*

The name Kuldana Formation was given by Latif [37] for a sequence of multi-colored shales at the base of the Murree Formation. The Kuldana Formation consists of variegated color shales, clays, siltstones and sandstones. The color of shales and clays are purple, greenish, yellowish and reddish maroon (Figure 3F). The dull purple, greyish green and purple are weathered colors of the shales and clays. The sandstone is hard, compact and fine-grained. The lower contact of the Kuldana Formation with the Chorgali Formation is conformable and has a gradational upper contact with the Murree Formation. The age of the Kuldana Formation is Middle to Late Eocene.

### *3.7. Murree Formation*

The cyclic sequence of sandstone, claystone and shales are titled in Murree Formation in the HKS and adjoining areas, as determined by Wadia [35], Calkins et al. [38], Ashraf and Chaudhary [39,40]. The Formation consists of alternate beds of sandstone and shales.

Sandstone is fine to medium grained and non-micaceous. The color of the sandstone is reddish and grey. The sandstone is hard, compact and shows cross-bedding, load casts and rip ups (Figure 3G). These sedimentary structures are helpful for the paleo-flow and younging direction of the strata. The sandstone is medium to thickly bedded and large. In the project area, the sandstone is highly fractured and jointed (Figure 3H). The shales are reddish maroon in color. The lower contact with the Kuldana Formation is gradational, and the upper contact with the Quaternary deposits is unconformable. The age of the Murree Formation is Early Miocene.

### *3.8. Quaternary Deposits*

The Quaternary deposits are the recent deposits. These deposits are classified as alluvial, colluvial and river terrace deposits. The alluvial deposits are in the form of alluvial fans and along the meanders of main streams (Figure 3I). The colluvial deposits are present in the study area as colluvial fans. These colluvial fans mainly consist of angular to sub-angular fragments of dolomite of the Muzaffarabad Formation. The river terrace deposits are horizontally bedded clays and gravels. These deposits are present as a blanket over the underlying Murree Formation. The existing drainage pattern of the study area cuts the river terrace deposits. These deposits in the area are cyclic in nature and present at different levels used for cultivation purposes (Figure 3I).

## 4. U-Pb Geochronology

### *4.1. Sampling and Methods*

Six samples representative of the key Cenozoic sequences were selected for detrital zircon U-Pb age dating (Figure 1C). Among the collected samples, two samples representing the late Paleocene Patala Formation (2017TP1 and 2017TP2), two samples representing the Early Middle Eocene Kuldana Formation (2017TP3 and 2017TP4) and two samples from the Miocene Murree Formation (2017TP5 and 2017TP6) were processed, analyzed and described as elaborated in U-Pb probability density plots.

The studied samples were crushed and treated for the separation of the detrital zircon grains using heavy liquids and magnetic separation techniques. The grains were then mounted in epoxy resin, and the zircon grain surface was polished to make the surface smooth. Finally, the surface of these mounted zircon grains was cleaned and washed with dilute Nitric Acid (HNO3) and pure alcohol for the removal of lead contamination before the in situ laser U-Pb analyses. The U-Pb analyses on detrital zircon grains were performed using the Agilent 7500a Quadruple Inductively Coupled Plasma Mass Spectrometer (Q-ICP-MS) attached with a NewWave UP 193 nm ArF excimer laser-ablation system at the Institute of Tibetan Plateau Research, Chinese Academy of Sciences. The analytical procedure for the zircon grains in this study was followed as described by Cai et al. [41].

One hundred mounted individual detrital zircon grains from each sample were analyzed except 2017TP2. From sample 2017TP2, only 90 zircon grains were analyzed. The zircon Plesovice was taken as an internal standard for the calibration of the unknown ages. The mean age of the Plesovice zircon is 337 $\pm$ 0.37 Ma [42]. The standard 91,500 was used as an external standard. The age of the 91,500 is 1064 $\pm$ 5 Ma [43]. The final ages of the individual zircon grains were assigned on the basis of $^{207}Pb/^{206}Pb$ and $^{206}Pb/^{238}U$ age systems. The $^{207}Pb/^{206}Pb$ age system opted for the zircon grains with ages >1000 Ma, while $^{206}Pb/^{238}U$ age system opted for zircon grains with ages <1000 Ma. The Glitter 4.0 software was used for the standardization of the U-Pb ages against standard zircon Plesovice (mean age of 337 $\pm$ 0.37 Ma) to process the raw data [42]. The zircon grains with <10% discordance were included in the final interpretation. For the illustration of detrital zircon grains regarding U-Pb ages, the probability density plots were developed by using ISOPLOT [44]. The zircon U-Pb detailed age data are provided in the supplementary data (Table S1).

### *4.2. U-Pb Detrital Zircon Results*

Two samples from the Late Paleocene Patala Formation were analyzed. One hundred (n = 100) detrital zircon grains were analyzed from sample 2017TP1, where 98 grains yielded usable ages (zircon grains with <10% age discordance) (Figure 4), out of which two populations are <290 Ma. The other prominent peaks vary between 510–984 Ma. In comparison, smaller peaks and scattered ages were present between 1000 Ma and 1500 Ma. The dominant peaks from data lie between 1500 Ma and 2000 Ma. The rest of the grains mostly show scattered ages between 2043–3428 Ma. The oldest age produced by the sample was 3428 ± 8 Ma, whereas the youngest age was 57 ± 1 Ma. Sample 2017TP2 from the Patala Formation generally shows a similar data set, where 86 grains with usable ages were selected out of 100 analyzed grains (Figure 4). The grains show a prominent peak around 130 Ma, whereas mild peaks were observed between 500–1000 Ma. A broad smaller peak was recorded between 1000 Ma and 2000 Ma. The oldest grain was 3011 ± 32 Ma, and the youngest grain had the age of 55 ± 2 Ma.

The two samples from the Early-Middle Eocene Kuldana Formation (2017TP3 and 2017TP4) were analyzed for U-Pb detrital zircon dating. The sample 2017TP3 with 99 detrital grains out of 100 showed results with ages having <100 Ma peaks (Figure 4). These clusters were mainly categorized into two groups, i.e., ranging from 39–56 Ma and 72–94 Ma prominent peaks. There was a range of detrital grains clustering between 102 Ma and 166 Ma. Other than that, the ages were scattered till 2500 Ma. The oldest detrital age recorded by a single grain was 2371 ± 11 Ma, and the youngest was 37.7 ± 0.3 Ma. The 2017TP4 sample from the Kuldana Formation with 96 selected grains out of 100 analyzed grains was used for the representation of the age data (Figure 4). The age spectrum was almost similar to the sample 2017TP3 age spectrum. The majority of the detrital grains yielded <200 Ma ages (Figure 4). The U-Pb probability density plot shows peaks with two groups of ages, i.e., 36–58 Ma and 60–100 Ma. The rest of the grains show the scattered age spectra ranging from 100–2600 Ma, where the oldest subjected age was 2605 ± 12 Ma, and the youngest was 35.9 ± 0.9 Ma.

The two samples from the Miocene Murree Formation (2017TP5 and 2017TP6) were analyzed for the U-Pb detrital zircon dating. The 2017TP5 sample from the Miocene Murree Formation with 100 detrital zircon grains gave 91 grains for usable ages (Figure 4). Generally, the ages were >100 Ma and showed random higher peaks between 400–1000 Ma. From 1000 Ma to 3000 Ma, the peaks were not so prominent. The ages found in between show scattered data. The oldest recorded detrital zircon age from this sample was 3012 ± 90 Ma, whereas the youngest one was 34.7 ± 1 Ma. The Miocene Murree Formation sample 2017TP6 was subjected to U-Pb analyses with 100 detrital zircon grains from which 95 grains were considered usable for the ages (Figure 4). Some of the grains peaked at 250 Ma, whereas most of the grains showed peaks between 430–950 Ma. In addition, the data presented some peaks between 1600–1800 Ma. The remaining data almost showed scattered ages between 2000 Ma and 3500 Ma. The oldest age from the zircon grain was 3235 ± 6 Ma, and the youngest recorded age was 22 ± 2 Ma.

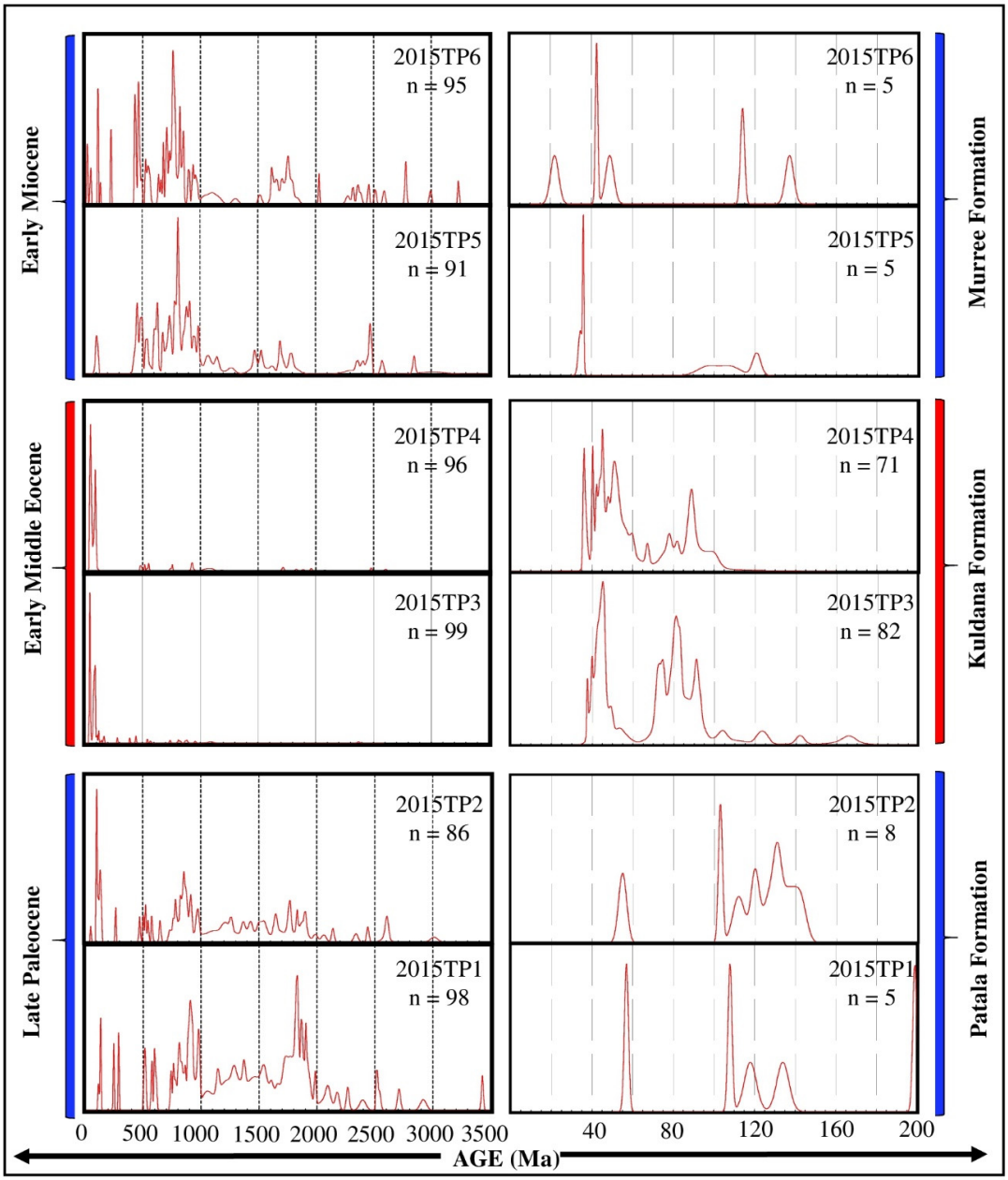


**Figure 4.** U-Pb probability density plots for studied samples of Late Paleocene Patala Formation, Early middle Eocene Kuldana Formation and Early Miocene Murree Formation, representing the Kotli section, Kashmir Basin, northwestern Himalaya, Pakistan.

## 5. Discussion

### *5.1. Detrital Zircon Provenance*

#### 5.1.1. U-Pb Ages of Source Terranes

The detrital zircon provenance interpretation for the upper Tertiary sequence that was exposed in the Yadgar section needs the U-Pb age data set representative for the litho-tectonic terranes, which were the possible source (contributing sediments) during the development of the Cenozoic foreland basin. The litho-tectonic terranes included are; Karakoram Block, Lhasa Block, Kohistan–Ladakh Island arc (KLA), Greater/Higher Himalaya, Lesser Himalaya and Tethyan Himalaya [1,45,46]. These terranes have distinct age spectra that provide an indication of the source region feeding the foreland basin (Figure 5).

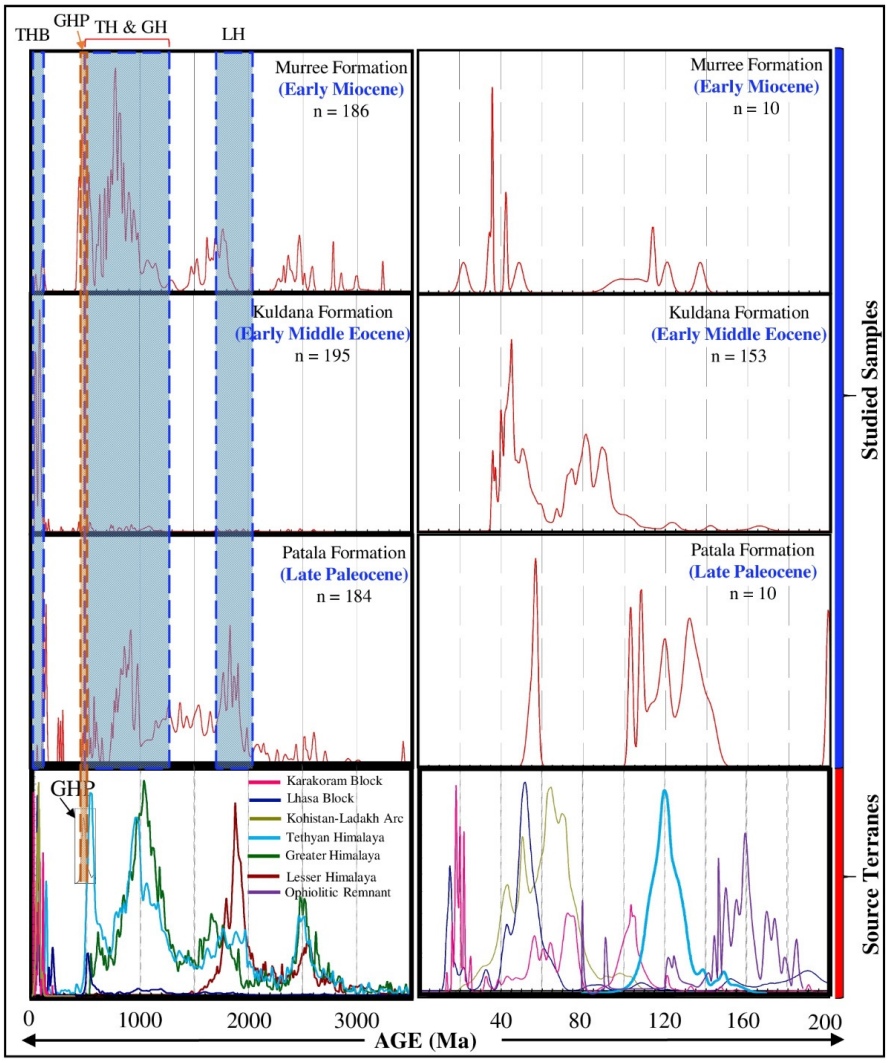


**Figure 5.** Comparison of composite U-Pb probability density plots Late Paleocene Patala Formation, Early-Middle Eocene Kuldana Formation and Early Miocene Murree Formation with the reference terranes (after Gehrels et al., [45]. The transparent rectangles depict the possible contribution of the various terranes. Where THB = Transhimalayan batholiths, GHP = Greater Himalayan Pluton, TH = Tethyan Himalayan, GH = Greater Himalayan and LH = Lesser Himalaya.

The lower, Lesser Himalaya gave a cluster of ages between 1700–1900 Ma from zircons with subordinate clustering between 2400–2600 Ma [45]. The Greater Himalayan Sequence (GHS) from the detrital zircons portray cluster ages between 540–750 Ma, 800–1200 Ma, 1600–1900 Ma and 2400–2600 Ma (Figure 5). The dominant ages of the GHS cluster ~900–1100 Ma [15,45]. The record of detrital zircon from the intruded granitic body shows cluster ages between 470–550 Ma along with a distinctive peak at 485 Ma [47]. The Tethyan and Upper-Lesser Himalayas have a similar detrital age spectra as the GHS. However, the age cluster of 480–570 Ma is relatively more prominent than other clusters, such as 700–1200 Ma and 2430–2560 Ma (Figure 5) [48–51]. The Tethyan strata also consists of younger detrital zircon grains having the age range between 110–140 Ma, which is representative of the volcanic rocks from the Indian Plate [13,15,45,52–54]. The ophiolitic remnants exposed at different localities along the Indus suture zone possess ages between ~115 and ~178 Ma [26,55]. The westernmost ophiolites (Bela-Muslim Bagh-Zhob, Waziristan and Dargai ophiolites) are stratigraphically emplaced over the Paleocene sediments and thus considered to be Late Cretaceous in age [19]. The MMT, northern collision zone in Pakistan, where the KLA represents the southern margin of the Eurasian Plate, is accreted to the Karakoram Plate. A recent study by Bouilhol, Jagoutz, Hanchar and Dudas [2] provided

a valuable dataset of U-Pb zircon ages for incorporation to interpret the identification of the sources from KLA. A broad age range between 40–110 Ma with some distinct peaks at 43 Ma, 50 Ma, 65 Ma and 70 Ma are shown for the KLA age spectra (Figure 5). In comparison, the Lhasa block granitic rocks, having the younger age spectra (Gangdese Batholith), yielded an age cluster of ~40–60 Ma with a distinct peak at 52 Ma and a significant population of ~18 Ma (Figure 4) [56]. The detrital zircons from the U-Pb age spectra of granitic rock bodies (Karakoram batholith) from the Karakoram Block showed clusters ~11–22 Ma with peaks at 18 Ma and 20 Ma, 53–80 Ma with dominant peaks at 56 Ma, 65 Ma and 73 Ma, and 93–110 Ma with a single peak at 103 Ma, respectively (Figure 5) [57–60].

#### 5.1.2. Sources to Tertiary Foreland Sequence

##### Patala Formation (~57–55 Ma)

Generally, the Patala Formation produced an age range with a cluster around <290 Ma with clustering segments showing peaks between ~130–290 Ma, ~500–1000 Ma and prominent peaks between ~1000 Ma and ~1500 Ma. There are minor scattered ages present between 2000 Ma and 3500 Ma (Figure 5). This discussed age pattern dominantly matches the Lesser Himalayan spectrum indicating the Indian Plate provenance (Figure 5). Both the samples show broadly similar age patterns. The detrital grains with ages between 130–290 Ma are representative of the ophiolitic source. The ophiolite emplacement in the late Cretaceous period was recently suggested in the western Himalayas [61]. This interpretation supports our ophiolitic component in the Patala Formation. This age spectrum resembles the Tethyan Himalayas and Lesser Himalayas, which indicates Indian Plate provenance with a minor contribution from the ophiolitic remnants. However, a substantial percentage (~11%) of Cretaceous–Paleocene detrital zircons were observed in the upper part of the Patala Formation. These younger grains are typically from the Kohistan-Ladakh Arc, which then accreted onto the Karakoram Batholith in the Late Cretaceous period and represented the southern margin of the Eurasian Plate to the north of the collision zone [58]. This contribution from the Kohistan-Ladakh Arc designates the mixing of Indian and Eurasian Plates provenance, which occurred during the upper Patala Formation deposition.

##### Kuldana Formation (~56–43 Ma)

The Kuldana Formation yielded age spectra with a distinctive cluster around <100 Ma, i.e., ~36–58 Ma, ~72–94 Ma and ~102–166 Ma, whereas scattered ages were also reported ranging up to ~2500 Ma (Figure 5). These age spectra show a mixed source from different terranes, including Trans-Himalayan batholiths, Tethyan Himalaya and Lower-Lesser Himalaya. The age spectra from the Tethyan Himalaya and Greater Himalaya are alike. However, the existence of a few Jurassic zircon grains strengthens the possible input of Tethyan Himalaya instead of GH because the GH was still buried under during the deposition of Eocene sequences [62]. The presence of abundant Cretaceous zircons shows that during the deposition of the Early-Middle Eocene Kuldana Formation, the dominant source was KLA with a possible contribution from the Karakoram block and Gangdese arc. Lithologically, it is the first sandy unit in the Kuldana Formation after the thick Paleocene–Eocene limestone sequence. Therefore, the Kuldana Formation indicates the detrital record with a mixed provenance of India and Eurasia. The only possibility for the contribution from the Karakoram and Lhasa blocks in the Kuldana Formation prevails when the KLA accreted first to these terranes and later on collided with the northern Indian margin. In this way, by considering the possible contribution as reflected by the similar age spectra, it fully supports the model of the first accretion of the KLA with the Karakoram block prior to the final collision with Indian Plate [23].

##### Murree Formation (~36.1–22 Ma)

The Kuldana Formation with a marine–continental transitional sequence is unconformably overlain by the continental deposits of the Murree Formation. The amalgamated

age spectra for the detrital samples from the Murree Formation show dominant age clusters >100 Ma, ~250–950 Ma and ~1000–1800 Ma (Figure 5). Subordinate age populations between ~1800–3000 Ma are also recorded. The straightforward contribution from these age clusters and peaks indicate various litho-tectonic terranes, including KLA, GH, LLH, TH and Upper-Lesser Himalaya. The GH sequence contribution is supported by the ~447–550 Ma cluster with a dominant peak at ~460 Ma, ~482 Ma and ~500 Ma, which prominently matched with the granitic gneisses of the GHS [47]. This detritus contribution from the GH sequence indicates that the GH was uplifted and exposed to provide the detritus for the evolving foreland basin. The contribution of the younger detrital zircon grains to the foreland basin was by the KLA, Karakoram block and Gangdese arc. The involvement of these various litho-tectonic terranes mentioned above evidenced the southward propagation of the fold–thrust belt as a consequence of the India–Eurasia collision.

### *5.2. Tectonic Implications*

The Cenozoic stratigraphic sequence was deposited during the transition of the northern Indian Plate margin from passive to active. Therefore, the Cenozoic stratigraphic sequence records the collisional process as well. In the northwestern Himalayas, the collisional timing of the Indian and Asian Plates was ~56 Ma [16,17]. During this time, the transition of the sediments occurred in the Patala Formation and became a more pronounced up-section in the Early-iMddle Eocene Kuldana Formation and Miocene Murree Formation (Figure 5). The detrital zircon provenance in this study provides an insight into the timing of collision. We proposed a tectonic evolution model relying on the detrital zircon provenance to explain the collision process (Figure 6). Our data suggest that the dominant provenance during the deposition of the Patala Formation is from the Indian craton. However, the younger detrital zircon with ages of 55 Ma and 57 Ma indicate derivation from the KLA. This contribution from the KLA indicates that in the western Himalayas, the India–Asia collision started at the end of the Paleocene period during 57–55 Ma (Figure 6A). In the up-section, the detrital zircon provenance of the Kuldana Formation shows the increased input from the KLA, and associated northern provenances may indicate the rapid exhumation of the KLA (Figure 6B). Similarly, the detrital provenance of the Murree Formation indicates an increased input from the KLA and also the Greater and Lesser Himalayan blocks that indicate the southward propagation of the Himalayan fold–thrust belt.

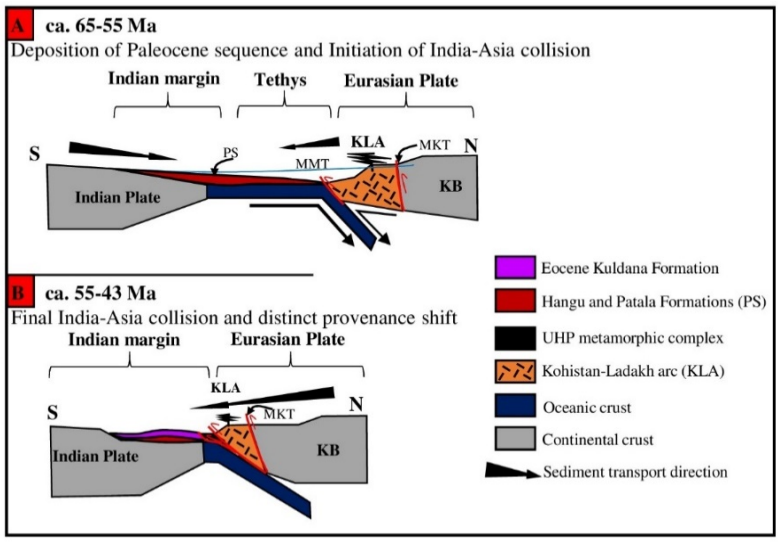


**Figure 6.** Tectonic model explaining the provenance change and India–Asia collision in the northwestern (NW) Himalayas (modified after Ding et al., [16]). (**A**) Deposition of the Paleocene sequence and initiation of the India–Asia collision. (**B**) Final India–Asia collision and subsequent exhumation of the KLA and associated blocks indicating major provenance shift from south to north.

## 6. Conclusions

This study resulted in the following conclusions;

1. The detrital zircon U-Pb ages show a major provenance change occurred in the upper part of the Patala Formation, which is more pronounced in the upper Tertiary Kuldana and Murree formations. This indicates that it is more likely associated with the India–Asia collision in northern Pakistan.
2. The mixed provenance in the Patala Formation suggest that the ophiolites exhumed during the Late Paleocene contributed the source to the evolving foreland basin together with Kohistan Island arc and the Indian craton.
3. This provenance change also suggests that the India–Asia collisional timing in the Kashmir basin, northwestern Himalaya, is constrained to be around 57–55 Ma considering the age of the Patala Formation.
4. The up-section, the mixed detritus in the Kuldana and Murree formations, indicate the exhumation of Greater and lesser Himalayan blocks in response to the southward propagation of a fold–thrust belt during the Eocene–Miocene period.

**Supplementary Materials:** The following are available online at https://www.mdpi.com/article/10.3390/min11121399/s1. Table S1. U-Pb isotopic analysis of detrital zircons.

**Author Contributions:** Funding acquisition, L.D.; investigation, M.A.; supervision, M.S.B. and S.P.; writing—original draft, M.Q.; writing—review and editing, J.I.T. and M.S. All authors have read and agreed to the published version of the manuscript.

**Funding:** This study was financially supported by grants from the National Natural Science Foundation of China (41490610), the Chinese Ministry of Science and Technology (2011CB403101) and the International partnership program of the Chinese Academy of Sciences (131551KYSB20200021).

**Institutional Review Board Statement:** Not Applicable.

**Informed Consent Statement:** Not Applicable.

**Data Availability Statement:** Data is available in supplementary file.

**Acknowledgments:** This study is part of a thesis carried out at the UAJK, Pakistan and PIFI postdoc research. We are thankful for the reviewers for their valuable input during the peer review.

**Conflicts of Interest:** The authors declare that there is no conflict of interest.

## References

1. Najman, Y. The detrital record of orogenesis: A review of approaches and techniques used in the Himalayan sedimentary basins. *Earth-Sci. Rev.* **2006**, *74*, 1–72. [CrossRef]
2. Bouilhol, P.; Jagoutz, O.; Hanchar, J.M.; Dudas, F.O. Dating the India–Eurasia collision through arc magmatic records. *Earth Planet. Sci. Lett.* **2013**, *366*, 163–175. [CrossRef]
3. Guillot, S.; Mahéo, G.; De Sigoyer, J.; Hattori, K.; Pecher, A. Tethyan and Indian subduction viewed from the Himalayan high-to ultrahigh-pressure metamorphic rocks. *Tectonophysics* **2008**, *451*, 225–241. [CrossRef]
4. Kaneko, Y.; Katayama, I.; Yamamoto, H.; Misawa, K.; Ishikawa, M.; Rehman, H.; Kausar, A.; Shiraishi, K. Timing of Himalayan ultrahigh-pressure metamorphism: Sinking rate and subduction angle of the Indian continental crust beneath Asia. *J. Metamorph. Geol.* **2003**, *21*, 589–599. [CrossRef]
5. Leech, M.L.; Singh, S.; Jain, A.; Klemperer, S.L.; Manickavasagam, R. The onset of India–Asia continental collision: Early, steep subduction required by the timing of UHP metamorphism in the western Himalaya. *Earth Planet. Sci. Lett.* **2005**, *234*, 83–97. [CrossRef]
6. Rehman, H.U.; Yamamoto, H.; Shin, K. Metamorphic P–T evolution of high-pressure eclogites from garnet growth and reaction textures: Insights from the Kaghan Valley transect, northern Pakistan. *Isl. Arc* **2013**, *22*, 4–24. [CrossRef]
7. Ahmad, M.N.; Yoshida, M.; Fujiwara, Y. Paleomagnetic study of Utror Volcanic Formation: Remagnetizations and postfolding rotations in Utror area, Kohistan arc, northern Pakistan. *Earth Planets Space* **2000**, *52*, 425–436. [CrossRef]
8. Zaman, H.; Otofuji, Y.-i.; Khan, S.R.; Ahmad, M.N. New paleomagnetic results from the northern margin of the Kohistan Island Arc. *Arab. J. Geosci.* **2013**, *6*, 1041–1054. [CrossRef]
9. Sun, Z.; Jiang, W.; Li, H.; Pei, J.; Zhu, Z. New paleomagnetic results of Paleocene volcanic rocks from the Lhasa block: Tectonic implications for the collision of India and Asia. *Tectonophysics* **2010**, *490*, 257–266. [CrossRef]

10. van Hinsbergen, D.J.; Lippert, P.C.; Li, S.; Huang, W.; Advokaat, E.L.; Spakman, W. Reconstructing Greater India: Paleogeographic, kinematic, and geodynamic perspectives. *Tectonophysics* **2019**, *760*, 69–94. [CrossRef]
11. van Hinsbergen, D.J.; Steinberger, B.; Doubrovine, P.V.; Gassmöller, R. Acceleration and deceleration of India-Asia convergence since the Cretaceous: Roles of mantle plumes and continental collision. *J. Geophys. Res. Solid Earth* **2011**, *116*, B06101. [CrossRef]
12. Bera, M.; Sarkar, A.; Chakraborty, P.; Loyal, R.; Sanyal, P. Marine to continental transition in Himalayan foreland. *Geol. Soc. Am. Bull.* **2008**, *120*, 1214–1232. [CrossRef]
13. Cai, F.; Ding, L.; Yue, Y. Provenance analysis of upper Cretaceous strata in the Tethys Himalaya, southern Tibet: Implications for timing of India–Asia collision. *Earth Planet. Sci. Lett.* **2011**, *305*, 195–206. [CrossRef]
14. Clyde, W.C.; Khan, I.H.; Gingerich, P.D. Stratigraphic response and mammalian dispersal during initial India-Asia collision: Evidence from the Ghazij Formation, Balochistan, Pakistan. *Geology* **2003**, *31*, 1097–1100. [CrossRef]
15. DeCelles, P.; Kapp, P.; Gehrels, G.; Ding, L. Paleocene-Eocene foreland basin evolution in the Himalaya of southern Tibet and Nepal: Implications for the age of initial India-Asia collision. *Tectonics* **2014**, *33*, 824–849. [CrossRef]
16. Ding, L.; Qasim, M.; Jadoon, I.A.; Khan, M.; Xu, Q.; Cai, F.; Wang, H.; Baral, U.; Yue, Y. The India–Asia collision in north Pakistan: Insight from the U–Pb detrital zircon provenance of Cenozoic foreland basin. *Earth Planet. Sci. Lett.* **2016**, *455*, 49–61. [CrossRef]
17. Qasim, M.; Ding, L.; Khan, M.A.; Jadoon, I.A.; Haneef, M.; Baral, U.; Cai, F.; Wang, H.; Yue, Y. Tectonic implications of detrital zircon ages from lesser Himalayan Mesozoic-Cenozoic strata, Pakistan. *Geochem. Geophys. Geosyst.* **2018**, *19*, 1636–1659. [CrossRef]
18. Najman, Y.; Carter, A.; Oliver, G.; Garzanti, E. Provenance of Eocene foreland basin sediments, Nepal: Constraints to the timing and diachroneity of early Himalayan orogenesis. *Geology* **2005**, *33*, 309–312. [CrossRef]
19. Beck, R.A.; Burbank, D.W.; Sercombe, W.J.; Riley, G.W.; Barndt, J.K.; Berry, J.R.; Afzal, J.; Khan, A.; Jurgen, H.; Metje, J. Stratigraphic evidence for an early collision between northwest India and Asia. *Nature* **1995**, *373*, 55–58. [CrossRef]
20. Bossart, P.; Ottiger, R. Rocks of the Murree Formation in northern Pakistan: Indicators of a descending foreland basin of late Paleocene to middle Eocene age. *Eclogae Geol. Helv.* **1989**, *82*, 133–165.
21. Najman, Y.; Pringle, M.; Godin, L.; Oliver, G. Dating of the oldest continental sediments from the Himalayan foreland basin. *Nature* **2001**, *410*, 194–197. [CrossRef]
22. Baig, M.; Lawrence, R. Precambrian to early Paleozoic orogenesis in the Himalaya. *Kashmir J. Geol.* **1987**, *5*, 1–22.
23. Searle, M.; Khan, M.; Fraser, J.; Gough, S.; Jan, M.Q. The tectonic evolution of the Kohistan-Karakoram collision belt along the Karakoram Highway transect, north Pakistan. *Tectonics* **1999**, *18*, 929–949. [CrossRef]
24. Coward, M.; Butler, R.; Khan, M.; Knipe, R. The tectonic history of Kohistan and its implications for Himalayan structure. *J. Geol. Soc.* **1987**, *144*, 377–391. [CrossRef]
25. Searle, M.; Treloar, P. Was Late Cretaceous–Paleocene obduction of ophiolite complexes the primary cause of crustal thickening and regional metamorphism in the Pakistan Himalaya? *Geol. Soc. Lond. Spec. Publ.* **2010**, *338*, 345–359. [CrossRef]
26. Ding, L.; Kapp, P.; Wan, X. Paleocene-Eocene record of ophiolite obduction and initial India-Asia collision, south central Tibet. *Tectonics* **2005**, *24*, TC3001. [CrossRef]
27. Gansser, A. *Geology of the Himalayas*; Interscience: London, UK, 1964.
28. Kazmi, A.H.; Jan, M.Q. *Geology and Tectonics of Pakistan*; Graphic Publishers: Karachi, Pakistan, 1997.
29. Nakata, T. Geomorphic history and crustal movement of the foot-hills of the Himalayas. *Sci. Rep. Tohoku Univ.* **1972**, *22*, 39–177.
30. Nakata, T. Active faults of the Himalaya of India and Nepal. *Geol. Soc. Am. Spec. Pap.* **1989**, *232*, 243–264.
31. Islam, M. Structure, stratigraphy, petroleum geology and tectonics of Mirpur, Khuiratta and Puti Gali areas of district Mirpur and Kotli, Azad Jammu and Kashmir. Pakistan. Unpublished MS Thesis, Institute of Geology, University of Azad Jammu and Kashmir, Muzaffarabad, Pakistan, 2006; p. 170.
32. Baig, M.; Snee, L. The evidence for Cambro-Ordovician orogeny in northwest Himalayas Pakistan. *Geol. Soci. Am.* **1995**, *27*, 305.
33. Waagen, W.H.; Wynne, A. *The Geology of Mount Sírban, in the Upper Punjâb*; Memoir of the Geological Survey of India: Calcutta, India, 1872.
34. Meddlicot, H. Notes on the sub-Himalayan series of Jammu Hills. *Rec. Geol. Surv. India* **1876**, *9*, 49.
35. Wadia, D. The syntaxis of the northwest Himalaya: Its rocks, tectonics and orogeny. *Rec. Geol. Surv. India* **1931**, *65*, 189–220.
36. Wadia, D.N. *The Geology of Poonch State (Kashmir) and Adjacent Portions of the Punjab*; Government of India Central Publication Branch: New Delhi, India, 1928.
37. Latif, M. Stratigraphy and micropaleontology of the Galis Group of Hazara, Pakistan. *Geol. Bull. Punjab Univ.* **1976**, *13*, 1–64.
38. Calkins, J.A.; Offield, T.W.; Abdullah, S.; Ali, S.T. *Geology of the Southern Himalaya in Hazara, Pakistan, and Adjacent Areas*; US Government Printing Office: Washington, DC, USA, 1975.
39. Ashraf, M.; Chaudhary, M. Petrology of lower Siwalik rocks of Poonch area. *Kashmir J. Geol.* **1984**, *2*, 1–10.
40. Ghazanfar, M.; Chaudhry, M.N. Reporting MCT in Northwest Himalaya, Pakistan. *Univ. Punjab Geol. Bull.* **1986**, *11*, 10–18.
41. Cai, F.; Ding, L.; Leary, R.J.; Wang, H.; Xu, Q.; Zhang, L.; Yue, Y. Tectonostratigraphy and provenance of an accretionary complex within the Yarlung–Zangpo suture zone, southern Tibet: Insights into subduction–accretion processes in the Neo-Tethys. *Tectonophysics* **2012**, *574*, 181–192. [CrossRef]
42. Sláma, J.; Košler, J.; Condon, D.J.; Crowley, J.L.; Gerdes, A.; Hanchar, J.M.; Horstwood, M.S.; Morris, G.A.; Nasdala, L.; Norberg, N. Plešovice zircon—a new natural reference material for U–Pb and Hf isotopic microanalysis. *Chem. Geol.* **2008**, *249*, 1–35. [CrossRef]

43. Yuan, H.-L.; Gao, S.; Dai, M.-N.; Zong, C.-L.; Günther, D.; Fontaine, G.H.; Liu, X.-M.; Diwu, C. Simultaneous determinations of U–Pb age, Hf isotopes and trace element compositions of zircon by excimer laser-ablation quadrupole and multiple-collector ICP-MS. *Chem. Geol.* **2008**, *247*, 100–118. [CrossRef]
44. Ludwig, K. *Isoplot/Ex 3: A Geochronological Toolkit Microsoft Excel*; Berkeley Geochronology Center: Berkeley, CA, USA, 2003.
45. Gehrels, G.; Kapp, P.; DeCelles, P.; Pullen, A.; Blakey, R.; Weislogel, A.; Ding, L.; Guynn, J.; Martin, A.; McQuarrie, N. Detrital zircon geochronology of pre-Tertiary strata in the Tibetan-Himalayan orogen. *Tectonics* **2011**, *30*, TC5016. [CrossRef]
46. Ravikant, V.; Wu, F.-Y.; Ji, W.-Q. U–Pb age and Hf isotopic constraints of detrital zircons from the Himalayan foreland Subathu sub-basin on the Tertiary palaeogeography of the Himalaya. *Earth Planet. Sci. Lett.* **2011**, *304*, 356–368. [CrossRef]
47. Cawood, P.A.; Johnson, M.R.; Nemchin, A.A. Early Palaeozoic orogenesis along the Indian margin of Gondwana: Tectonic response to Gondwana assembly. *Earth Planet. Sci. Lett.* **2007**, *255*, 70–84. [CrossRef]
48. Aikman, A.B.; Harrison, T.M.; Lin, D. Evidence for Early (>44 Ma) Himalayan Crustal Thickening, Tethyan Himalaya, southeastern Tibet. *Earth Planet. Sci. Lett.* **2008**, *274*, 14–23. [CrossRef]
49. Myrow, P.; Hughes, N.; Paulsen, T.; Williams, I.; Parcha, S.; Thompson, K.; Bowring, S.; Peng, S.-C.; Ahluwalia, A. Integrated tectonostratigraphic analysis of the Himalaya and implications for its tectonic reconstruction. *Earth Planet. Sci. Lett.* **2003**, *212*, 433–441. [CrossRef]
50. Myrow, P.M.; Hughes, N.C.; Goodge, J.W.; Fanning, C.M.; Williams, I.S.; Peng, S.; Bhargava, O.N.; Parcha, S.K.; Pogue, K.R. Extraordinary transport and mixing of sediment across Himalayan central Gondwana during the Cambrian–Ordovician. *Geol. Soc. Am. Bull.* **2010**, *122*, 1660–1670. [CrossRef]
51. Myrow, P.M.; Hughes, N.C.; Searle, M.P.; Fanning, C.; Peng, S.-C.; Parcha, S. Stratigraphic correlation of Cambrian–Ordovician deposits along the Himalaya: Implications for the age and nature of rocks in the Mount Everest region. *Geol. Soc. Am. Bull.* **2009**, *121*, 323–332. [CrossRef]
52. DeCelles, P.; Gehrels, G.; Najman, Y.; Martin, A.; Carter, A.; Garzanti, E. Detrital geochronology and geochemistry of Cretaceous–Early Miocene strata of Nepal: Implications for timing and diachroneity of initial Himalayan orogenesis. *Earth Planet. Sci. Lett.* **2004**, *227*, 313–330. [CrossRef]
53. Garzanti, E. Stratigraphy and sedimentary history of the Nepal Tethys Himalaya passive margin. *J. Asian Earth Sci.* **1999**, *17*, 805–827. [CrossRef]
54. Hu, X.; Garzanti, E.; Moore, T.; Raffi, I. Direct stratigraphic dating of India-Asia collision onset at the Selandian (middle Paleocene, 59 $\pm$ 1 Ma). *Geology* **2015**, *43*, 859–862. [CrossRef]
55. Kakar, M.I.; Kerr, A.C.; Mahmood, K.; Collins, A.S.; Khan, M.; McDonald, I. Supra-subduction zone tectonic setting of the Muslim Bagh Ophiolite, northwestern Pakistan: Insights from geochemistry and petrology. *Lithos* **2014**, *202*, 190–206. [CrossRef]
56. Ji, W.-Q.; Wu, F.-Y.; Chung, S.-L.; Li, J.-X.; Liu, C.-Z. Zircon U–Pb geochronology and Hf isotopic constraints on petrogenesis of the Gangdese batholith, southern Tibet. *Chem. Geol.* **2009**, *262*, 229–245. [CrossRef]
57. Fraser, J.E.; Searle, M.P.; Parrish, R.R.; Noble, S.R. Chronology of deformation, metamorphism, and magmatism in the southern Karakoram Mountains. *Geol. Soc. Am. Bull.* **2001**, *113*, 1443–1455. [CrossRef]
58. Heuberger, S.; Schaltegger, U.; Burg, J.-P.; Villa, I.M.; Frank, M.; Dawood, H.; Hussain, S.; Zanchi, A. Age and isotopic constraints on magmatism along the Karakoram-Kohistan Suture Zone, NW Pakistan: Evidence for subduction and continued convergence after India-Asia collision. *Swiss J. Geosci.* **2007**, *100*, 85–107. [CrossRef]
59. Jain, A.K.; Singh, S. Tectonics of the southern Asian Plate margin along the Karakoram Shear Zone: Constraints from field observations and U–Pb SHRIMP ages. *Tectonophysics* **2008**, *451*, 186–205. [CrossRef]
60. Ravikant, V.; Wu, F.-Y.; Ji, W.-Q. Zircon U–Pb and Hf isotopic constraints on petrogenesis of the Cretaceous–Tertiary granites in eastern Karakoram and Ladakh, India. *Lithos* **2009**, *110*, 153–166. [CrossRef]
61. Qasim, M.; Ding, L.; Khan, M.A.; Baral, U.; Jadoon, I.A.K.; Umar, M.; Imran, M. Provenance of the Hangu Formation, Lesser Himalaya, Pakistan: Insight from the detrital zircon U-Pb dating and spinel geochemistry. *Palaeoworld* **2020**, *29*, 729–743. [CrossRef]
62. DeCelles, P.G.; Gehrels, G.E.; Quade, J.; LaReau, B.; Spurlin, M. Tectonic Implications of U-Pb Zircon Ages of the Himalayan Orogenic Belt in Nepal. *Science* **2000**, *288*, 497–499. [CrossRef]